Fallick A.E., McConville P., Boyce A.J., Burgess R. & Kelley S.P., 1992- Laser microprobe stable isotope measurements on geological materials: some experimental considerations (with special reference to (34S in sulfides)), Chemical Geology, 101: 53-61.

Geological Survey of Iran, 1992, Geological map of Torbat Heidarieh (scale 1:250,000).

Germann K., Lüder V., Banks D.A., Simon K. & Hoefs J., 2003- Late Hercynian polymetallic vein-type base-metal mineralization in the Iberian Pyrite Belt: fluid-inclusion and stable-isotope geochemistry (S-O-H-Cl), Mineralium Deposita, 38: 953-967.

Hoefs J., 2004- Stable Isotope Geochemistry, Springer-Verlog, Berlin, 244 p.

John D., Hofstra A.H., Fleck R.J., Brummer J.E. & Saderholm E.C., 2003- Geologic setting and genesis of the Mule Canyon low sulfidation epithermal gold-silver deposit, North-Central Nevada, Economic Geology, 98: 425-463.

Keivanfar M. & Asgari A., 2000- Explanatory text of geological map of Arghash district (scale 1:5000): Geological Survey of Iran, 81 p, (in Persian).

Kelley S.P. & Fallick A.E., 1990- High precision spatially resolved analysis of d34S in sulfides using a laser extraction technique, Geochimica et Cosmochimca Acta, 54: 883-888.

Lensch G., Mihm A. & Alavi-Tehrani N., 1977- Petrography and geology of the ophiolite belt north of Sabzevar/Khorasan (Iran), Neues Jahrbuch Fur Geologie un Palaontologie Monatshefte, 131: 156-178.

Lindenberge H.G., Gorler K. & Ibbeken H., 1983- Stratigraphy, structure and orogenic evolution of the Sabzevar zone in the area of Oryan (Khorasan, NE Iran), Geological Survey of Iran Report 51, p. 119-143.

McCrea J.M., 1950- On the isotopic chemistry of carbonates and a paleotemperature scale, Journal of Chem. Physics, 18: 849-857.

McKibben M.A. & Eldridge C.S., 1990- Radical sulfur isotope zonation in pyrite accompanying boiling and epithermal gold deposition: a SHRIMP study of the Valles Caldera, New Mexico, Economic Geology, 85: 1917-1925.

Ohmoto H. & Goldhaber M.B., 1997- Sulfur and carbon isotopes. In: Barnes H.L. (eds.) Geochemistry of hydrothermal ore deposits, John Wiley and Sons, pp. 517-611.

Ohmoto H. & Rye R.O., 1979- Isotopes of sulfur and carbon. In: Barnes H.L. (eds.) Geochemistry of Hydrothermal Ore Deposits, John Wiley and Sons, pp. 509-567.

Ohmoto H., 1972- Systematics of sulfur and carbon isotopes in hydrothermal ore deposits, Economic Geology, 67: 551-578.

Ronacher E., Richards J.P., Reed M.H., Bray C.J., Spooner E.T.C. & Adams P.D., 2004- Characteristics and evolution of the hydrothermal fluid in the north zone high-grade area, Porgera gold prospect, Papua New Guinea, Economic Geology, 99: 843-867.

Sengor A.M.C., 1990- A new model for the Late Paleozoic-Mesozoic tectonic evolution of Iran and implications for Oman. In: Robertson, A.H.F., Searle, M.P., Ries, A.C., (eds.) The Geology and Tectonics of the Oman Region, Geological Society of London Special Publication 49, pp. 797-831.

Shelton K.L., So C.S., Haeussler G.T., Chi S.J. & Lee K.Y., 1990- Geochemical studies of the Tongyoung gold-silver deposits, Republic of Korea: Evidence of meteoric water dominance in a Te-bearing epithermal system, Economic Geology, 85: 1114-1132.

So C.S., Chi S.J., Shelton K.L. & Skinner B.J., 1985- Copper-bearing hydrothermal vein deposits in the Gyeongsang basin, Republic of Korea, Economic Geology, 80: 43-56.

Spies O., Lensch G. & Mihm A., 1983- Geochemistry of the post-ophiolitic Tertiary volcanics between Sabzavar and Quchan/NE-Iran: Geological Survey of Iran, Report No.51, p. 247-267.

Thiersch P.C., Williams-Jones A.E. & Clark J.R., 1997- Epithermal mineralization and ore controls of the Shasta Au-Ag deposit, Toodoggone district, British Columbia, Canada, Mineralium Deposita, 32: 44-57.

TOZCO, 2001- Regional geological map of Arghash area, Geological Survey of Iran.

Wagner T., Boyce A.J. & Fallick A.E., 2002- Laser combustion analysis of δ34S of sulfosalt minerals: determination of the fractionation systematics and some crystal-chemical considerations, Geochimica et Cosmochimica Acta, 66: 2855-2863.

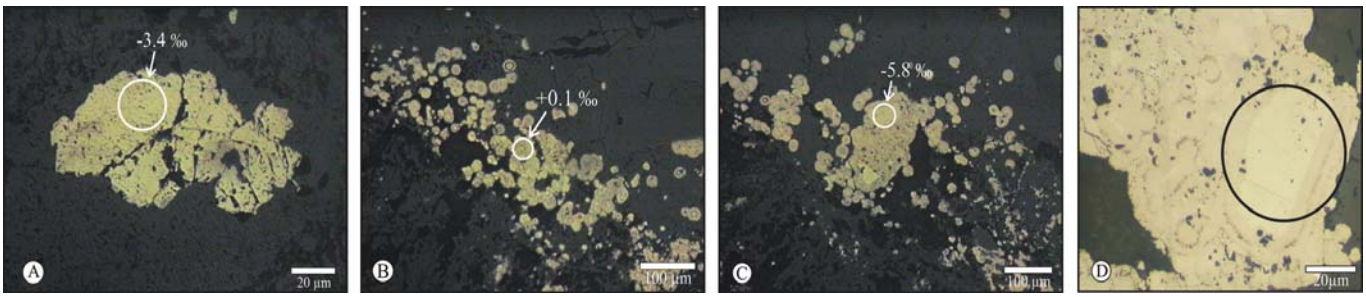

FIG. 2- Microphotographs showing the locations of the laser spots in various generations of pyrites. A. Fine- to coarse-grained pyrite (Py-I); B. Framboidal pyrite (Py-II). C. Arsenian overgrowth pyrite (Py-III). Circles represent the location of laser spots. The $\delta^{34}S$ values (in per mil) are indicated. Sample is from drill core ZK001-2 in Au-III vein system at 98 m from surface. D. Zoom view of C.

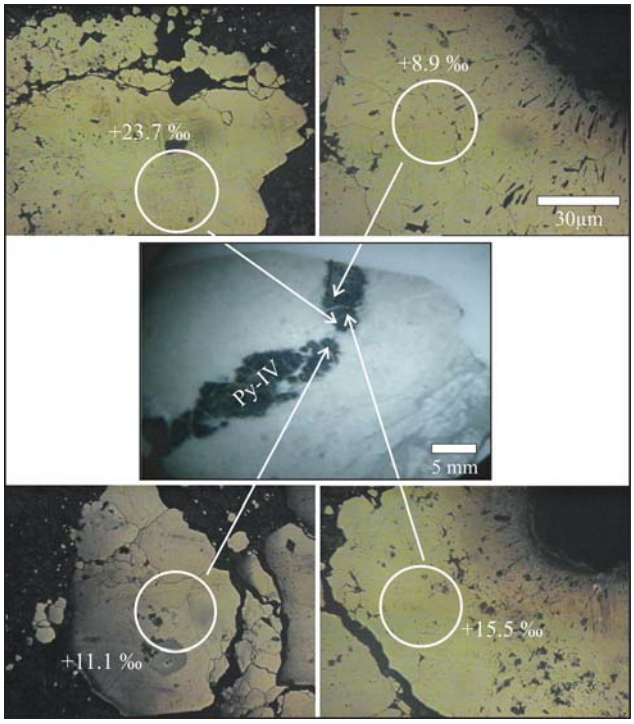

FIG. 3- Microphotographs showing the locations of the laser microprobe spots in Py-IV. The isotopic values (in per mil) of each spot are shown on photos. Circles represent the location of laser spots. Sample is from drill cores ZK1602-28 in Au-III vein system at 61 m from surface.

References

Ahmad M., Solomon M. & Walshe J.L., 1987- Mineralogical and geochemical studies of the Emperor gold telluride deposit, Fiji, Economic Geology, 82: 345-370.

Camus F., Boric R., Skewes M.A., Castelli J.C., Reichhard E. & Mestre A., 1991- Geologic, structural, and fluid inclusion studies of El Bronce epithermal vein system, Petorca, Central Chile, Economic Geology, 86: 1317-1345.

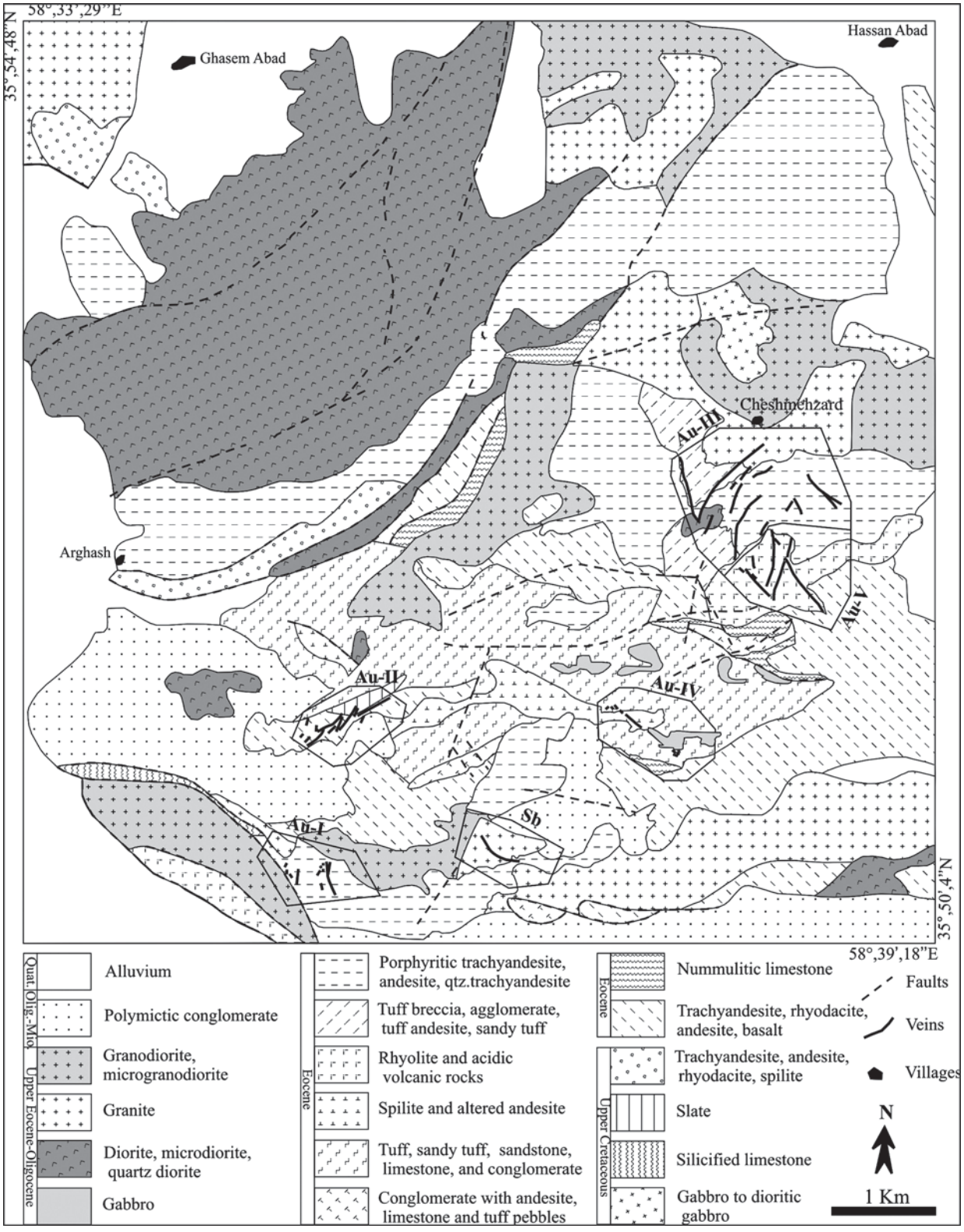

FIG. 1- Geological map of Arghash gold district (modified after TOZCO, 2001). The locations of the vein systems Au-I to Au-V and the stibnite vein are indicated.

Table 1. Summary of sulfur, carbon, and oxygen isotope values in per mil for samples from drill cores and surface veins in various vein systems.

Sample No.	X	Y	Vein system (depth)	δ34S‰	δ13C‰	δ18O‰	Mineral
AR6-180	35º 50' 35"	58º 36' 28"	Sb (-)	-18.8	-		Stibnite vein
AR6-181	35º 50' 29"	58º 36' 37"	Sb (-)	-14.4	-		Stibnite vein
ZK2301-4	-	-	Au-III (67)	-4.3	-		Disseminated Py
ZK1101-7	-	-	Au-III (74)	-4	-		Disseminated Py
ZK1602-7	-	-	Au-II (82)	-3.8	-		Fracture-filling Py
ZK2301-11	-	-	Au-III (132)	-3.7	-		Disseminated Py
ZK3202-7	-	-	Au-IV (45)	+5.1	-		Disseminated Py
ZK1602-18	-	-	Au-II (60)	+9.3	-		Fracture-filling Py
ZK1602-22	-	-	Au-II (53)	+12.2	-		Fracture-filling Py
ZK1602-2	-	-	Au-II (78)	+13.4	-		Fracture-filling Py
ZK3202-15	-	-	Au-III (66)	+13.5	-		Disseminated Py
ZK1101-9	-	-	Au-III (32)	+21.8	-		Disseminated Py
ZK1101-11	-	-	Au-I (65)	-	1.6	22.9	Calcite vein
ZK001-1	-	-	Au-III(89)	-	1.2	14.0	Calcite vein
ZK001-2	-	-	Au-III (98)	-	1.3	15.1	Calcite vein
ZK002-7	-	-	Au-II (83)	-	0.8	14.1	Calcite vein
ZK4301-3	-	-	Au-III (10)	-	12.0	29.8	Calcite vein

Sulfur data are relative to CDT, oxygen data to SMOW and carbon data to PBD. Samples prefixed by AR are from surface samples, whereas those prefixed by ZK are drill core samples. The depth of the core samples are shown in parenthesis in meter. X and Y show latitudes and longitudes for surface samples. Py: pyrite.

strata occur in the Paleozoic and Mesozoic basement units.

The $\delta^{18}O$ values of the calcites vary between +14.0 to +29.8 per mil (Table 1). This range in association with oxygen and hydrogen isotope compositions of quartz and kaolinite suggest that hydrothermal waters were of meteoric origin, and that experienced a complex history of mixing, prolonged water/rock interaction, and boiling.

6. Conclusion

(1) Four generations of pyrite occur in Arghash vein systems. Py-I to Py-III are associated with gold, and Py-IV is barren. Sulfur isotope values for ore stage pyrites are consistent with derivation of sulfur from a magma or older igneous rocks; $\delta^{34}S$ values for Py-IV suggest abstraction of sulfur from enriched sources, like sulfate bearing beds. Such beds occur locally in the Eocene and older sedimentary units in south and southwest of Arghash district.

(2) The $\delta^{34}S$ values of two stibnites sharply contrast with those of the pyrites, suggesting a different source for sulfur and Sb, and possibly a different hydrothermal history.

(3) Carbon isotope data suggest that hydrothermal fluids obtained CO_2 from dissolution or decarbonation of carbonate rocks by circulation along faults and fractures (cf. Ahmad et al., 1987; John et al., 2003; Ronacher et al., 2004).

(4) The isotopic data suggest that hydrothermal fluids experienced a complex history of water/rock interaction; ore constituents were extracted through leaching of country rocks along permeable zones. Gold deposition occurred primarily during boiling process, which is supported by crustiform banding, chalcedony veinlets, bladed calcite, abundant calcite veins, and breccia textures. Water/rock interaction also played an important role in gold deposition; this is supported by the occurrence of gold in altered wall rocks adjacent to veins.

Acknowledgement

This research was funded by the Ministry of Sciences, Research, and Technology of Iran, and by a Natural Sciences and Engineering Research Council of Canada Discovery research grant and University of Saskatchewan Department Head Research Support Program grant to Kevin M. Ansdell. Review by H. Mirnejad from University of Tehran improved the manuscript.

than 0.5 per mil variation in the $\delta^{34}S$ of the precipitating pyrite (Ohmoto & Goldhaber, 1997). In H_2S-dominated systems, the fO_2 and pH do not play an important role in the sulfur isotope variation, and accordingly, the $\delta^{34}S$ values of sulfides would be similar to $\delta^{34}S\Sigma S$ of the ore fluid (Ohmoto, 1972; German et al., 2003). The ore and alteration mineralogy (pyrite-dominant and lack of sulfate minerals) in Arghash vein systems are consistent with an H_2S-dominated hydrothermal system.

Boiling and subsequent H_2S loss could cause ^{34}S-enrichment in the precipitating sulfides (McKibben and Eldrige, 1990). Py-IV formed during the waning stages of hydrothermal processes; it is barren of gold, and clearly late in paragenesis. Enrichment in ^{34}S can not be attributed to boiling.

Considering the wide variations in the $\delta^{34}S$ values, and the marked contrast in the isotopic compositions between the two groups of pyrites (Py-IV compared to Py-I to Py-III), source area and/or variable physicochemical conditions during vein formation may account for sulfur isotope variations within the two groups. The $\delta^{34}S$ values in conventional bulk analyses, not detected in laser probe experiments, could be due to the fact that bulk samples contain different generations of pyrites.

A magmatic source, or derivation of sulfur from older igneous rocks, during circulation of the hydrothermal fluids, is proposed for the origin of sulfur in Py-I to Py-III in laser probe experiments ($\delta^{34}S$ = +0.1 to -5.8‰) and in bulk analyses ($\delta^{34}S$ = +5.1 to -4.3‰) (cf. So et al., 1985; Shelton et al., 1990; Camus et al., 1991; Thiersch et al., 1997).

The high $\delta^{34}S$ values in both bulk analyses and laser probe (Py-IV) may reflect contributions of isotopically heavy sulfur from a source enriched in ^{34}S, like evaporites. Gypsum, anhydrite, gypsiferous marl, and halite-bearing beds occur locally in the Eocene and older sedimentary units in south and southwest of Arghash district (Geological Survey of Iran, 1992). Reduction of aqueous sulfate to aqueous sulfide could take place thermogenically, or through reactions with Fe^{+2}-bearing minerals; sulfate-bearing waters could thus evolve into sulfide-bearing hydrothermal fluids (Ohmoto and Rye, 1979, Ohmoto and Goldhaber, 1997).

The sulfur isotope ratios of two stibnites from the quartz-stibnite vein in granite ($\delta^{34}S$=-18.8 and -14.4‰) sharply contrast with those of the pyrites from Au-I–Au-V vein systems, suggesting a different sulfur, and possibly metal source, and/or radical changes in the physicochemical conditions of the fluid during deposition of stibnite. Sulfur and antimony might have been extracted from metasedimentary basement rocks by the granitic magma or circulating fluids; alternatively, changes in fO_2 at the site of deposition could lead to extremely depleted sulfides due to SO_2 loss or formation of sulfate minerals (cf. Ohmoto and Goldhaber, 1997; Germann et al., 2003). The quartz-stibnite veins are free of sulfate minerals, and evidence for changes in fO_2 of the fluids, i.e. reactions with oxidizing wall rocks, are lacking. The sulfur isotope characteristics of the stibnites are best explained by source effects.

Except for one sample, the $\delta^{13}C_{PDB}$ values of the calcites are near 1 per mil (Table 1) which is typical of marine carbonates (cf. Hoefs, 2004). Carbonate units and interlayers in the area, that are variably silicified and recrystallized, are a suitable source for the CO_2 in the ore fluids (cf. Ahmad et al., 1987; John et al., 2003). The $\delta^{13}C$ of one sample is +12.0 per mil. Such carbon isotope signatures may be attributed to local decreases in the mole ratios of CO_2/CH_4 in the fluid (cf. Ohmoto and Goldhaber, 1997). Separation of CH_4 would lead to enrichment of ^{13}C in the remaining CO_2 in the hydrothermal fluid. Decreases in the CO_2/CH_4 mole ratios could occur through reactions of CO_2-rich fluids with carbonaceous materials. Organic-rich

to 1980 ppm Au (Ashrafpour, 2007); (4) Fracture-filling, anhedral, barren, late stage pyrite (Py-IV).

4. Analytical Procedures

Sulfur isotope analyses were performed on bulk materials as well as on single grains. For bulk materials, twelve samples were analyzed using a Thermo Finnigan DeltaPlus IRMS at the G.G. Hatch Stable Isotope Laboratories, University of Ottawa. The sulfur isotope data are presented in delta notation relative to the CDT (Canion Diablo Triolite) standard ($\delta^{34}S_{CDT}$‰). The standard error of analyses is less than ±0.2 per mil.

For single grains, in-situ laser combustion analyses were performed on two polished slabs from Au-III vein system at the Scottish Universities Environmental Research Center (SUERC) using a SPECTRON LASERS 902Q CW Nd-YAG laser (1W power), operating in TEM00 mode, following the method of Fallick et al. (1992). The released SO_2 gas was purified in a vacuum line, which operates similar to a conventional sulfur extraction line (Kelley and Fallick, 1990). The analytical precision, based on replicate analyses of the standards, was around ±0.2 per mil.

The spatial resolution is dictated by the amount of SO_2 gas the mass spectrometer requires for analysis of isotope ratios. Determination of the sulfur isotope composition of SO_2 was carried out online by a VG SIRA II mass spectrometer, which requires a minimum of 0.05-0.10 µmol SO_2. This corresponds to a spot size of 50 to 100µm. The details of the technique are outlined by Wagner et al. (2002).

To constrain the source(s) of CO_2 in ore fluids, five representative samples from vein calcites, collected from drill cores, were analyzed for $\delta^{13}C$ and $\delta^{18}O$ values at the G.G. Hatch Stable Isotope Laboratories, University of Ottawa. CO_2 gas was extracted through reaction of 500µg samples with H_3PO_4 following McCrea (1950), and analyzed by a Thermo Finnigan DeltaPlus XP IRMS. The analytical precision is ±0.1 per mil.

5. Discussion

Bulk analyses were carried out on 10 pyrite-bearing samples from auriferous veins and adjacent altered wall rocks, as well as two stibnites (Table 1); no distinction was made between various generations of pyrites at this stage. $\delta^{34}S$ values for the pyrites vary from -4.3 to +21.8 per mil; the two stibnites are -14.4 and -18.8 per mil (Table 1). The $\delta^{34}S$ values for pyrites fall into two groups, one highly enriched in ^{34}S (+9.3 to +21.8‰), and the other less enriched to slightly depleted in ^{34}S (+5.1 to -4.3‰). These values represent various combinations of different generations of pyrite and can not be used for source interpretations. As shown earlier, four generations of pyrites were identified (Py-I to Py-IV); three generations, Py-I to Py-III, are associated with gold and one generation, Py-IV, is barren. An in-situ laser combustion technique was employed to characterize the isotopic compositions of various generations of pyrites.

The $\delta^{34}S$ values for Py-I to Py-III vary between -5.8 to +0.1 per mil (Fig. 2); this is comparable to $\delta^{34}S$ values for the second group in the bulk analyses. Py-IV is highly enriched in ^{34}S ($\delta^{34}S$= +8.9 to +23.7‰) (Fig. 3). This accounts for the high $\delta^{34}S$ values (+9.3 to +21.8‰) in the bulk sulfur experiments. The sulfur isotope composition of sulfides is controlled by the source area, physicochemical conditions (temperature, fO_2, pH) during hydrothermal processes, and depositional mechanism (boiling) (e.g. Ohmoto, 1972; McKibben and Eldrige, 1990; Ohmoto and Goldhaber, 1997). The effect of physicochemical conditions on isotopic composition is variable and depends on the dominant sulfur species in the hydrothermal fluid, as H_2S-dominated fluids will yield restricted isotopic variations (Ohmoto, 1972; Ohmoto & Goldhaber, 1997).

A temperature decrease from 350º to 150ºC causes less

oldest rocks in the district include small outcrops of Upper Cretaceous ophiolites (Keivanfar & Asgari, 2000), consisting of gabbro to diorite-gabbro, silicified limestone, slate, variably altered volcanic rocks, and spilitic pillow lavas (Fig. 1).

Tertiary volcanic activity started in Lower-Middle Eocene with eruption of andesitic, trachyandesitic, andesitic basalt, and rhyodacitic lavas (TOZCO, 2001 ; Keivanfar & Asgari, 2000); they are locally associated with nummulitic limestone and conglomerate. The volcanic rocks are covered by Middle Eocene pyroclastic rocks, including tuffs and sandy tuffs, and minor sandstone, nummulitic limestone, and conglomerate. Spilitic lavas and altered andesites form a distinct mappable unit in the pyroclastic rocks. The pyroclastic volcanic activity extended into the Upper Eocene; this is represented by tuff breccias, agglomerates, tuffs, andesite, andesitic tuffs and sandy tuff in the west and southwest of Cheshmehzard village (Fig. 1). Upper Eocene silicic volcanic rocks (rhyolite) are intensively altered and form small outcrops only in the east and south of the district.

The volcanic activity ended in Upper Eocene by eruption of porphyritic trachyandesite, quartz-trachyandesite, and andesite. Granite, granodiorite, and diorite bodies of Upper Eocene-Oligocene age intruded into volcanic rocks in the north and south of the district (Keivanfar and Asgari, 2000). Intensive alteration in the Arghash district is mainly confined to 1 to 5 m from the veins. Wall rocks are partially to completely replaced by clay minerals and Fe oxides-hydroxides. Argillic alteration is well developed within and away from the ore-related alteration zones. Post-ore alteration oxidized sulfides to Fe-oxides-hydroxides above water table.

3. Ore Mineralization

Arghash district includes five gold-bearing vein systems, Au-I to Au-V, and one antimony-rich vein (Sb) (Fig. 1). Mineralization occurred as fracture-filling veins with local occurrences of hydrothermal breccias, and disseminations and veinlets in the immediate wall rocks. The veins consist mostly of quartz and carbonates. They are hosted mostly by intermediate to silicic volcanic rocks, tuffs, granite, and diorite (Fig. 1).

The veins vary in length from 350 m to more than 1.2 km and in thicknesses from 0.5 to 5 m. Breccias, chalcedony veinlets, bladed calcite, crustiform textures, and quartz-calcite intergrowths are common. Maximum assays obtained from many trenches and drill cores for Au, Ag, As, Sb, and Hg are 83, 220, 19600, 2730, and 6.2 g/t, respectively. The Au-III is the main ore system. Antimony ore vein consists of intimate association of stibnite and grey to dark quartz along a fault in granite. Stibnite ore occurs as scattered patches and bands, 1-10 cm thick, throughout the vein.

All vein systems show similar ore and hydrothermal alteration assemblages. Pyrite is the main sulfide mineral in the hypogene ore. Four generations of pyrite were identified through detailed microscopic observations and electron microprobe analyses (Figs. 2 and 3):

(1) Euhedral to anhedral fine- to coarse-grained pyrite (Py-I), associated with quartz in veins as well as in the wall rocks. The pyrite is locally accompanied by minor chalcopyrite, marcasite, tetrahedrite-tennantite, and arsenopyrite. Native gold grains occur in quartz associated with the pyrite; (2) Framboidal pyrite (Py-II) occurring as scattered grains, 10-30 μm in diameter, and in aggregates in microfractures in quartz and calcite. The pyrite is characterized by concentric bands of grey (As-poor) and white (As-rich) materials, containing up to 960 ppm Au (Ashrafpour, 2007); (3) Arsenian pyrite overgrowths (Py-III) occurring as rims <10 μm thick on euhedral to anhedral pyrites of Py-I; the pyrite contains up

conventional bulk analyses fall into two groups, one highly enriched in ^{34}S ($\delta^{34}S$= +9.3 to +21.8‰), and the other less enriched to slightly depleted in ^{34}S ($\delta^{34}S$= +5.1 to -4.3‰). In-situ laser probe experiments were carried out to characterize various generations of pyrite. The results indicate a relatively narrow range for Py-I to Py-III (δ34S= -5.8 to +0.1‰) consistent with a magmatic source for sulfur. Py-IV is highly enriched ($\delta^{34}S$= +8.9 to +23.7‰), implying contributions of sulfur from sources enriched in ^{34}S, like evaporites. The high $\delta^{34}S$ values in the enriched group can be attributed to a significant occurrence of Py-IV in this group.

The $\delta^{34}S$ values of two stibnites from Sb ore (-18.8 and -14.4‰) suggest a different sulfur, and possibly metal source, and/or radical changes in the physicochemical conditions of the fluid during deposition of stibnite. Metasedimentary basement rocks could contribute sulfur and metal to the circulating fluids. $\delta^{13}C_{PDB}$ values of vein calcites are near 1 per mil suggesting a sedimentary source for carbon. Carbonate units and interlayers in the area are a suitable source for CO_2 in the ore fluids. The stable isotope data suggest that hydrothermal fluids experienced a complex history of water/rock interaction and that ore components, were derived, at least partly, from country rocks.

Keywords: Arghash, Gold, Pyrite, Stibnite, Sulfur, Carbon, Isotope.

1. Introduction

Stable isotopes have become an integral part of ore deposit studies, playing an important role in understanding ore genesis (Ohmoto,1972; Ohmoto & Rye, 1979; Hoefs, 2004). Stable isotope studies on epithermal systems have indicated the involvement of variable sources for hydrothermal fluids and ore metals.

Advances in the isotope ratio analytical techniques now allow discrimination among the many events that occur during the history of hydrothermal systems. In this research, variations in sulfur and carbon isotope compositions of vein materials (pyrite, stibnite, and calcite) from Arghash gold district, and their bearings to the fluid sources, physicochemical conditions, and by extrapolation, sources of metals, are investigated.

2. Geological Setting

Arghash gold district is located in Sabzevar zone in northern margin of the Central Iranian Microcontinent. The basement of the Sabzevar zone consists of Precambrian metamorphosed rocks covered by Paleozoic epicontinental sediments. An extensional regime between Central Iranian Microcontinent and southern margin of Eurasia in Jurassic-Cretaceous (Lindenberg et al.,1983)formed a narrow branch of Neo-Tethys, known as Sabzevar Ocean (Sengor,1990). Subduction of the oceanic crust under East Alborz belt in Late Cretaceous to Tertiary lead to the development of a magmatic arc (Spies et al.,1983). Sabzevar ophiolites are considered as remnants of the oceanic crust emplaced during Upper Cretaceous (Lensch et al.,1977).

Tertiary volcanic rocks are widespread, particularly in the southern part of the eastern segment of the Sabzevar zone; they can be divided into Eocene andesitic group, Oligocene to Pliocene dacitic group, and Late Oligocene-Miocene alkaline group(Spies et al.,1983). Several Tertiary plutonic bodies comprising granite to granodiorite intruded older rocks.

Arghash gold district is located at latitude 35º 50' 4"N, longitude 58º 39' 18"E, approximately 45 km southwest of Neishabour in northeastern Iran. The

تغییرات ایزوتوپی گوگرد، کربن و اکسیژن در سولفید و کربنات در محدوده طلای ارغش، جنوب باختر نیشابور، شمال‌خاور ایران

نوشته: اسماعیل اشرف‌پور*، کوین م. انسدال و سعید علیرضایی***

*گروه زمین‌شناسی، دانشگاه شهید بهشتی، تهران، ایران
**گروه زمین‌شناسی، دانشگاه ساسکاچوان، کانادا

Sulfur, Carbon and Oxygen Isotope Variations of Sulfide and Carbonate in Arghash Gold Prospect, Southwest Neishabour, Northeastern Iran

By: E. Ashrafpour*, K. M. Ansdell & S. Alirezaei***

*Department of Geology, University of Shahid Beheshti, Tehran, Iran
**Department of Geology, University of Saskatchewan, 114 Science Place, Saskatoon, SK, S7N 5E2, Canada

تاریخ دریافت : ۱۲/ ۰۷ / ۱۳۸۵ تاریخ پذیرش : ۳۰ / ۰۲ / ۱۳۸۶

چکیده

محدوده طلای ارغش شامل پنج سامانه رگه‌ای طلادار (Au-I تا Au-V) و یک رگه آنتیموان‌دار است. سنگ میزبان این رگه‌ها، سنگ‌های آتشفشانی اسیدی تا حدواسط، توف، گرانیت و دیوریت است. پیریت کانی سولفیدی اصلی و شامل چهار نسل مختلف (Py-I تا Py-IV) است. مقادیر $\delta^{34}S$ پیریت‌ها در تجزیه‌های ماده کل، شامل یک گروه بسیار غنی از ^{34}S ($\delta^{34}S$: ۹/۳+ تا ۲۱/۸+ در هزار) و یک گروه کمی غنی تا کمی تهی شده از ^{34}S ($\delta^{34}S$: ۵/۱+ تا ۴/۳- در هزار) است. برای تعیین ویژگی ایزوتوپی نسلهای مختلف پیریت‌ها تجزیه‌های ریزکاو(پروب) لیزری صورت گرفت. پیریت‌های نسل اول تا سوم گستره به‌نسبت کوچکی از $\delta^{34}S$ ($\delta^{34}S$: ۵/۸- تا ۰/۱+ در هزار) نشان می‌دهند که می‌تواند نشانگر منشأ ماگمایی برای گوگرد باشد. پیریت‌های نسل چهارم بسیار غنی از ^{34}S هستند (۸/۹+ تا ۲۳/۷+ در هزار) که حاکی از تأمین گوگرد از یک منشأ غنی از ^{34}S مانند تبخیری‌ها است. مقادیر بالای $\delta^{34}S$ در پیریت نسل چهارم مسئول مقادیر مثبت $\delta^{34}S$ در تجزیه‌های ماده کل هستند.

مقادیر $\delta^{34}S$ دو نمونه استیبنیت از کانسنگ آنتیموان (۱۴/۴- تا ۱۸/۸- در هزار) می‌تواند مربوط به منشأ متفاوت گوگرد و احتمالاً آنتیموان و/یا تغییرات شدید در شرایط فیزیکوشیمیایی سیال در هنگام نهشت کانسنگ باشد. پی‌سنگ رسوبی- دگرگونی می‌تواند تأمین‌کننده گوگرد و آنتیموان باشد. مقادیر $\delta^{13}C_{PDB}$ حدود ۱ در هزار نمونه‌های کلسیت، نشان‌دهنده منشأ رسوبی کربن است. واحدها و میان لایه‌های کربناتی می‌توانند منشأ مناسبی برای کربن باشند. داده‌های ایزوتوپ‌های پایدار نشان می‌دهد که سیال‌های گرمابی تاریخچه پیچیده‌ای از برهم‌کنش سیال/سنگ را پشت سر گذاشته‌اند.

کلید واژه‌ها : ارغش، طلا، پیریت، استیبنیت، گوگرد، کربن، ایزوتوپ.

Abstract

Arghash gold district includes five gold-bearing vein systems, (Au-I to Au-V) and one antimony-rich vein hosted by intermediate to silicic volcanic rocks, tuffs, granite, and diorite. Pyrite is the main sulfide mineral consisting of four generations (Py-I to Py-IV). Py-I to III are intimately associated with gold; however, Py-IV is barren. The $\delta^{34}S$ values of pyrites in